ARTICLE IN PRESS

Available online at www.sciencedirect.com

SCIENCE DIRECT

Physica B 383 (2006) 63–66

PHYSICA B

www.elsevier.com/locate/physb

Comparison of the electronic structures of two non-cuprate layered transition metal oxide superconductors

E.R. Ylvisaker, K.-W. Lee, W.E. Pickett*

Department of Physics, University of California, Davis, CA 95616, USA

Abstract

Comparison is made of the electronic structure of the little-studied layered transition metal oxide $LiNbO_2$ with that of Na_xCoO_2, which has attracted tremendous interest since superconductivity was discovered in its hydrate. Although the active transition metal d states are quite different due to different crystal fields and band filling, both systems show a strong change of electronic structure with changes in the distance between the transition metal ion layer and the oxygen layers. The niobate is unusual in having a large second-neighbor hopping amplitude, and a nearest-neighbor hopping amplitude that is sensitive to the Nb–O separation. Li_xNbO_2 also presents the attractive simplicity of a single band triangular lattice system with variable carrier concentration that is superconducting.
© 2006 Elsevier B.V. All rights reserved.

PACS: 71.20.Be; 71.20.Dg; 74.25.Jb

Keywords: Electronic structure; Niobate; Sodium cobaltate; Superconductivity

1. Motivation

Among the various areas of research that were stimulated by the discovery of high temperature superconductors (HTS) nearly two decades ago is that of two-dimensional (2D) (or nearly so) transition metal oxides (TMOs). A second surprise appeared in 2001 with the discovery [1] of $T_c = 40\,K$ in MgB_2, where the physics is entirely different but the 2D character is crucial [2,3] for the surprisingly high value of critical temperature T_c. A further stimulus for study of superconductivity in 2D TMOs was provided in 2003 with the discovery of superconductivity [4] in hydrated Na_xCoO_2 at 4.5 K. These discoveries suggest a more general look at superconducting 2D TMOs besides the cuprates, to try to identify trends (or perhaps lack of trends).

Being isostructural to the first HTS $(La,Sr)_2CuO_4$, the ruthenate Sr_2RuO_4 has a special status in this class. Its electronic structure is quite distinct from that of HTS, however, and T_c is only around 1 K. There is now a very large literature on Sr_2RuO_4. It is a different and very perplexing superconductor, but we will not pursue it in this paper.

What we focus on here is the little-noticed layered TMO superconductor Li_xNbO_2, with brief comparison with the cobaltate system Na_xCoO_2. This niobate was discovered [5] in 1990 when the community was absorbed with the new HTS materials, and has not yet attracted the attention that it deserves. While its $T_c = 5.5\,K$ is quite close to that of the hydrated cobaltates (4.5 K) it is the contrasts that we will focus on. These differences revolve mainly on: 4d versus 3d ion, trigonal versus octahedral coordination by six oxygen neighbors, and single band versus multiband character. We expose one similarity: z-displacement of the oxygen layers, which modulates the TM–oxygen distance, has a strong influence on the electronic structure.

2. Layered lithium niobate

The compound $LiNbO_2$ itself is a band insulator with gap ~2 eV. The de-lithiated phase Li_xNbO_2 was found by the Berkeley group to be superconducting [6], with the few reports to date suggesting superconductivity sets in around $x \approx 0.8$ (i.e., when 20% of the Li is removed) beyond which

*Corresponding author. Tel.: +1 530 753 4123; fax: +1 530 752 4717.
E-mail address: pickett@yclept.physics.ucdavis.edu (W.E. Pickett).

0921-4526/$ - see front matter © 2006 Elsevier B.V. All rights reserved.
doi:10.1016/j.physb.2006.03.057

T_c does not depend much on the Li content x. The structure of $LiNbO_2$ consists of a triangular lattice of both the Li cations and the transition metal (niobium) ions, separated by layers of oxygen atoms, similar to Na_xCoO_2 except for the TM coordination. The trigonal prismatic coordination of niobium atoms by oxygen ions provides a big distinction. The trigonal crystal field results in an energetic lowering of the Nb d_{z^2} states with respect to the other 4d states by about 4 eV, leaving the system with only a single band per formula unit to consider. This valence-conduction band is also well separated from the O 2p bands below (see Fig. 1).

Removal of the lithium has the effect of adding holes to the conduction band made up of Nb d_{z^2} states. Superconductivity appears, as it does when holes are introduced into $NaCoO_2$ (followed by hydration), and at a very similar temperature (5 K), but apparently at quite different carrier concentrations and for very different electronic structures. Since the Li content is variable, this compound becomes a clean representation of a single band triangular lattice system which can be compared rather directly with Hubbard model results. As part of our study of this system, we obtain a tight-binding (TB) representation of the band to allow the subsequent study of possible correlation effects within the Hubbard model. We return to these issues below.

Structure. $LiNbO_2$ takes on a hexagonal structure [6–8] ($a = 2.90$ Å, $c = 10.46$ Å) having space group $P6_3/mmc$ (No. 194), with sites Li [$2a(0, 0, 0), \bar{3}m$], Nb [$2d(\frac{2}{3}, \frac{1}{3}, \frac{1}{4}), \bar{6}m2$], and O [$4f(\frac{1}{3}, \frac{2}{3}, z_O), 3m$]. The oxygen internal parameter z_O specifies the Nb–O bond length and due to the stacking type there are two $LiNbO_2$ layers per cell. The distance between Nb atoms, a, is almost identical to bond length 2.86 Å in elemental BCC Nb, so direct Nb–Nb overlap should be kept in mind. Experimental values [6–9] of the internal parameter range from 0.125 to 0.129. Our optimization by energy minimization using the abinit code gives the value $z_O = 0.125$ (lattice constants held at the experimental values).

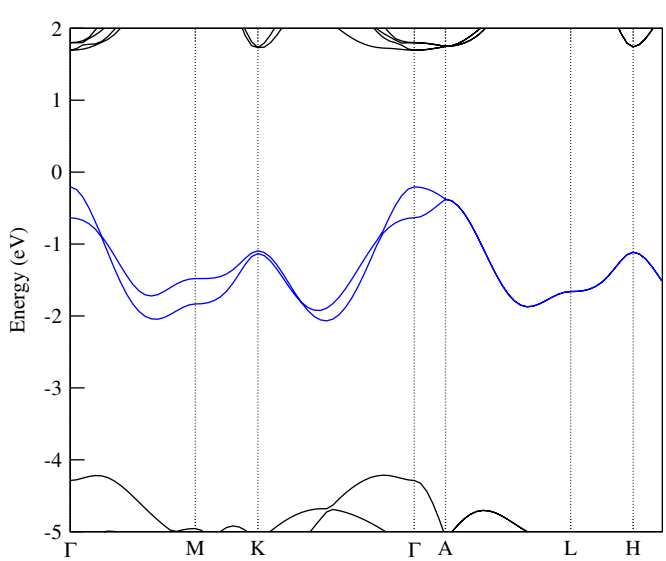

Fig. 1. Band structure for $z_O = 0.1263$ (one of the experimental values, slightly larger than our optimized value of 0.125), calculated using the code *abinit* [13]. Symmetry dictates that the two band stick together along the A–L–H–A lines ($k_z c = \pi$). Non-monotonicity of the bands along the A–L and A–H directions reflects the strong deviation from a nearest-neighbor hopping behavior as discussed further in the text. The crystal field splitting of the Nb 4d bands is ~4 eV.

Electronic structure and tight-binding representation. The band structure of $LiNbO_2$ pictured in Fig. 1 is similar to that given earlier by Novikov et al. [10] and indicates a Nb d_{z^2} bandwidth of 1.9 eV. The Nb d_{z^2}-O 2p bands can be fit straightforwardly to a TB model based on orthonormal Wannier functions on the two Nb atoms per cell (one Nb per layer). A full description of the results will be given elsewhere [22], but we provide a synopsis here. There are three important features of the TB fit that we emphasize here. First, a good fit requires rather long range hoppings, up to fourth neighbors within the layer and to three neighbors in the layers above and below. Second, with oxygen ions at their equilibrium position, the second-neighbor (in-plane) hopping amplitude $t_2 \approx 100$ meV is much larger than the nearest-neighbor hopping $t_1 \approx 60$ meV. The smaller value of t_1 may reflect interference between direct Nb–Nb interaction and the standard O-mediated Nb–O–Nb processes. The same trend has been observed for 2H–TaS_2 [11], where the small value of t_1 was traced to phase cancellation in the hopping integral when Wannier functions are on nearest neighbors. This $t_2 > t_1$ feature may have important implications for the microscopic understanding of the properties of Li_xNbO_2, since if t_2 were the only non-zero hopping, the system decomposes into three decoupled triangular lattices with lattice constant $\sqrt{3}a$; t_1 then becomes the "perturbation" that couples the three sublattices, breaks symmetry and removes degeneracy. Thirdly, the nearest-neighbor hopping t_1 is very strongly modulated by oxygen displacement. We find that t_1 increases strongly as the O layers "squash" against the Nb layers, as in the A_g Raman mode. This modulation may provide the largest contribution to electron–phonon coupling in this compound.

Effective charges. We have evaluated the Born effective charge tensor as described by Gonze and Lee [12] using the *abinit* code [13]. Given in Table 1 are the two distinct elements of the effective charge tensor for each atom type, calculated in the relaxed atomic structure together with the formal charges. Z^*_{xx}(Li) ($Z^*_{yy} = Z^*_{xx}$) is close to the formal charge of Li indicating primarily ionic type bonding for motion in the x–y plane, consistent with its propensity for de-intercalation. The charge tensor for Li shows similar anisotropy to that of LiBC [14] which is similar structurally and electronically (if some Li is de-intercalated) to the 40 K superconductor MgB_2. In LiBC $Z^*_{xx}(\text{Li}) = 0.81$, $Z^*_{zz}(\text{Li}) = 1.46$, and it was concluded that Li is involved in electronic coupling (not only ionic, but covalent) between consecutive B–C layers. Similar Li involvement might be expected in $LiNbO_2$, and indeed the band structure shows clear effects of interlayer coupling. The difference from the formal

Table 1
Born effective charges for $LiNbO_2$, together with a comparison with $NaCoO_2$ calculated by Li et al. [15]

	$LiNbO_2$			$NaCoO_2$		
	Li	Nb	O	Na	Co	O
Z^*_{xx}	1.10	2.26	−1.68	0.87	2.49	−1.68
Z^*_{zz}	1.69	1.31	−1.50	1.37	0.87	−1.12
Z^*_{av}	1.30	1.94	−1.62	1.04	1.95	−1.49
Z^0	+1	+3	−2	+1	+3	−2

The angular average Z^*_{av} is also displayed. Note the unexpected deviations from the formal values Z^0 of the effective charges for Li and Nb in the z-direction (larger for Li, smaller for Nb). For O in $LiNbO_2$, the effective charges are nearly isotropic. Overall, the anisotropies are rather similar in $NaCoO_2$, but somewhat more pronounced.

charges for the Nb ions (formally Nb^{3+}, O^{2-}) indicates substantial covalent character to the bonding which appears to be especially strong for z displacement of the Nb ion.

The Born effective charges have been reported [15] for $NaCoO_2$, and since we investigate O squashing in this compound in the next section, we have included the $NaCoO_2$ effective charges in Table 1 for comparison. Indeed there are several similarities, as noted in the table caption.

3. Layered sodium cobaltates

There is already a substantial literature on the electronic structure of the Na_xCoO_2 system. Briefly: the t_{2g} bands are broken in symmetry by the layered structure and by the squashing of the CoO_2 layers away from ideal cubic coordination by the six O ions. The bands are doped with $1-x$ holes, with all the evidence indicating the holes go, at least initially, into a_g states rather than e'_g states. Using the observed structure, it is found that this results from the somewhat larger a_g bandwidth, because the band centers remain indistinguishable.

We address here the effect of the height of the O ions above/below the Co layer. In the calculations, the full-potential non-orthogonal local-orbital minimum-basis scheme (FPLO) was used [16]. For specific doping levels and treatments of the Na ions, the height has been optimized by a number of groups [17–21], revealing that there is some sensitivity of the O position to the environment. To clarify the question of the effect of squashing without reference to a specific doping level, we display in Fig. 2 the t_{2g} bands for O height (from the Co layer) of 1.14 Å (corresponding to undistorted CoO_6 octahedra), 0.96 Å (typical value for intermediate values of x), and 0.88 Å (the smallest value reported). For orientation, we note that Johannes et al. [18] using the virtual crystal approximation for the Na concentrations $x = 0.3$, 0.5 and 0.7, obtained the heights 0.88, 0.90, 0.93 Å, respectively. The corresponding projected densities of states are shown in Fig. 3. For these calculations we used $x = 0.5$, treated within the virtual crystal model. To avoid unphysical O–O interactions across the layers as the O layer position was varied, the c axis was artificially increased by 20% for these calculations.

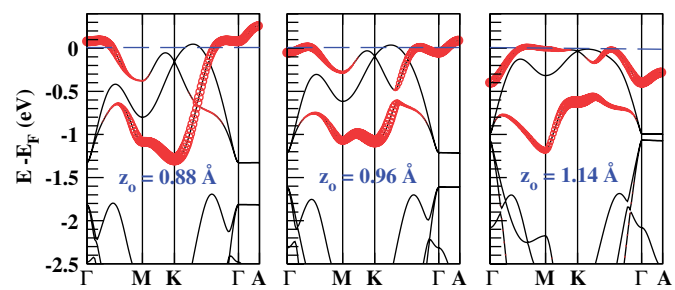

Fig. 2. The t_{2g} bands (which lie above −1.5 eV in these figures) of paramagnetic $Na_{0.5}CoO_2$ for three values of the O height z_O. The value 1.14 Å corresponds to symmetric CoO_6 octahedra. The thickened line emphasizes the a_g character. The changes in the t_{2g} bands are discussed in the text. Note also the changes in the O 2p bands just below the t_{2g} bands.

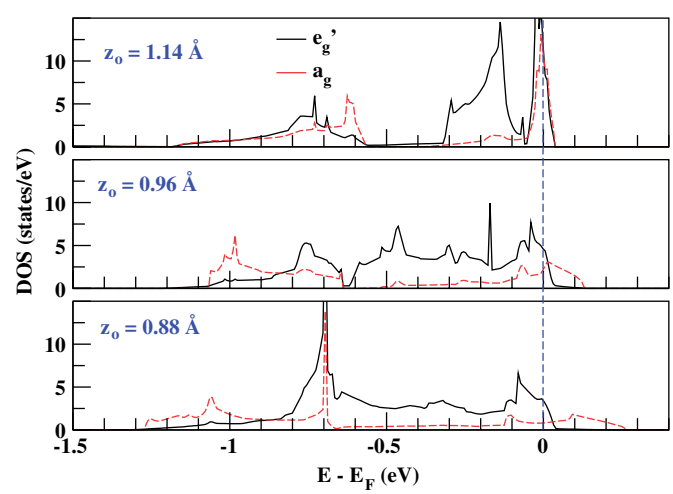

Fig. 3. The a_g and e'_g densities of states for the oxygen heights, and bands shown in Fig. 2. Note that the band widths are identical for the symmetric octahedra ($z_O = 1.14$ Å) but the 2D dispersion already results in a strongly differing DOS in the upper regions (where, within a rigid band picture, the doped holes reside).

Simple crystal field arguments would suggest: (1) for the cubic octahedron $z_O = 1.14$ Å the a_g and e'_g DOS should be the same, and (2) as the O ions are squashed down, the e'_g states should rise relative to the a_g states. The first expectation is severely violated in the region just below

E_F due to the dispersion being only 2D (presuming crystal fields from ions beyond nearest O ions are negligible). In addition, the effects of squashing are much more complex than suggested by the crystal field model. There is minor change in the mean energies of the a_g and e'_g states (they remain essentially equal, see Fig. 3), the main change is an *increase* in the a_g bandwidth compared to that of the e'_g states upon squashing. For $z_O = 1.14\,\text{Å}$, doped holes initially would go equally into each band. At the highly squashed end, ~0.4 holes/per Co can go into the a_g band before encountering the e'_g states. We emphasize that this is a model, constrained result; self-consistency and geometrical relaxation will change the details. There is also the question of decreasing interaction with the O 2p states upon squashing. This change which is of course also included in the changes shown in Figs. 2 and 3, may affect the a_g and e'_g states differently.

The changes in the band structure, Fig. 2 are more instructive. At Γ, the a_g state is almost 0.5 eV below its maximum for the cubic octahedron $z_O = 1.14\,\text{Å}$, the maxima occurring midway along both Γ–M and Γ–K lines. The additional structure, and the associated decrease in bandwidth reflects longer range hopping, and most likely a strong change in the ratio t_2/t_1, analogous to the changes in $LiNbO_2$ but with additional complications due to the presence of the e'_g bands. The shift with squashing motion in the e'_g bands is noticeable not only at Γ, where the state increases in energy, but also in the degeneracy at the K point, which rises to the top of the t_{2g} bands for the symmetric CoO_6 octahedron.

4. Summary

In this paper we have briefly compared and contrasted the electronic structure of the little-studied layered TMO $LiNbO_2$ to that of Na_xCoO_2, which has attracted tremendous attention since superconductivity was discovered in its hydrate. Although the active states are quite different, both systems show a strong change of electronic structure with changes in the TM–oxygen distance. The niobate is unusual in having a large second-neighbor hopping amplitude, and it also presents the attractive simplicity of a single active band on a triangular lattice. One of the primary questions to address is whether electronic correlations are important in the delithiated system, and whether the origin of superconductivity is of electronic or lattice origin.

Acknowledgments

We acknowledge stimulating comments from D. Khomskii and R. J. Cava on the effect of oxygen "squashing" in the Na_xCoO_2 system, and clarification from M. D. Johannes on calculations relating to this question. This work was supported by National Science Foundation Grant DMR-0421810.

References

[1] J. Nagamitsu, N. Nakagawa, T. Muranaka, Y. Zenitani, J. Akimitsu, Nature (London) 410 (2001) 63.
[2] I.I. Mazin, V.P. Antropov, Physica C 385 (2003) 49.
[3] W.E. Pickett, Brazilian J. Phys. 33 (2003) 695.
[4] K. Takada, Y. Sasago, E. Takayama-Muromachi, F. Izumi, R.A. Dilanian, T. Sasaki, Nature (London) 422 (2003) 53.
[5] M.J. Geselbract, T.J. Richardson, A.M. Stacy, Nature 345 (1990) 324.
[6] M.J. Geselbracht, A.M. Stacy, A.R. Garcia, B.G. Slibernagel, G.H. Kwei, J. Phys. Chem. 97 (1993) 7102.
[7] E.G. Moshopoulou, P. Bordet, J.J. Capponi, Phys. Rev. B 59 (1999).
[8] G. Meyer, R. Hoppe, Angew. Chem. (Int. Ed.) 13 (1974).
[9] A.P. Tyutyunnik, V.G. Zubkov, D.G. Kellerman, V.A. Pereliaev, A.E. Kar'kin, Eur. J. Solid State Inorg. Chem. 33 (1996) 53.
[10] D.L. Novikov, V.A. Gubanov, V.G. Zubkov, A.J. Freeman, Phys. Rev. B 43 (1994) 15830.
[11] R.L. Barnett, A. Polkovnikov, E. Demler, W.-G. Yin, W. Ku, Phys. Rev. Lett. 96 (2006) 026406.
[12] X. Gonze, C. Lee, Phys. Rev. B 55 (1997) 10355.
[13] X. Gonze, J.-M. Beuken, R. Caracas, F. Detraux, M. Fuchs, G.-M. Rignanese, L. Sindic, M. Verstraete, G. Zerah, F. Jollet, et al., Comput. Mater. Sci. 25 (2002) 478 The ABINIT code is a common project of the Université Catholique de Louvain, Corning Incorporated, and other contributors (URL http://www.abinit.org).
[14] K.-W. Lee, W.E. Pickett, Phys. Rev. B 68 (2003) 085308.
[15] Z. Li, J. Yang, J.G. Hou, Q. Zhu, Phys. Rev. B 70 (2004) 144518.
[16] K. Koepernik, H. Eschrig, Phys. Rev. B 59 (1999) 1743.
[17] P. Zhang, W. Luo, V.H. Crespi, M.L. Cohen, S.G. Louie, Phys. Rev. B 70 (2004) 085108.
[18] M.D. Johannes, D.A. Papaconstantopoulos, D.J. Singh, M.J. Mehl, Europhys. Lett. 68 (2004) 433.
[19] J. Ni, G. Zhang, Phys. Rev. B 69 (2004) 214503.
[20] Z. Li, J. Yang, J.G. Hou, Q. Zhu, Phys. Rev. B 71 (2005) 024502.
[21] K.-W. Lee, W.E. Pickett, Phys. Rev. B 72 (2005) 115110.
[22] E.R. Ylvisaker, W.E. Pickett, cond-mat/0602227.